Research Square

Preprints are preliminary reports that have not undergone peer review.
They should not be considered conclusive, used to inform clinical practice,
or referenced by the media as validated information.

Combined exposure to copper and polypropylene microplastics alters metal partitioning, chlorophyll homeostasis and phenylpropanoid metabolism in Nymphaea ‘Black Beauty’

Yuhong Rong
Yunnan Institute of Tropical Crops
Hongjun Mu
Yunnan Institute of Tropical Crops
Ziyu Li
Yunnan Institute of Tropical Crops
Zhaohao Zhang
Yunnan Institute of Tropical Crops
Jiang Xie
Yunnan Institute of Tropical Crops
Yongbo Zhang
Yunnan Institute of Tropical Crops
Yanyin Xu
Yunnan Institute of Tropical Crops
Shen Xiong
Yunnan Institute of Tropical Crops
Zesen Lai
Yunnan Institute of Tropical Crops
Haiying Xiong
Yunnan Institute of Tropical Crops
Kaixiong Li
Yunnan Institute of Tropical Crops
Shanman Li
College of Life Science, Guizhou University
Chao Luo
chaoluo@gzu.edu.cn

College of Life Science, Guizhou University

Research Article

Keywords: polypropylene microplastics, copper, Nymphaea‘Black Beauty’, chloroplast homeostasis, phenylpropanoid metabolism

Posted Date: June 26th, 2026

DOI: https://doi.org/10.21203/rs.3.rs-9970127/v1

License: This work is licensed under a Creative Commons Attribution 4.0 International License. Read Full License

Additional Declarations: No competing interests reported.

Version of Record: A version of this preprint was published at BMC Plant Biology on October 4th, 2026. See the published version at https://doi.org/10.1186/s12870-026-09848-1.

Abstract

Background

Microplastics can modify metal behavior in aquatic environments, but how polypropylene (PP) microplastics influence copper (Cu) partitioning and plant stress responses remains poorly understood. This study investigated the physiological, elemental, transcriptomic, and metabolomic responses of Nymphaea ‘Black Beauty’ to Cu, PP, and combined Cu-PP exposure.

Results

This study examined physiological, elemental, transcriptomic, and metabolomic responses of Nymphaea ‘Black Beauty’ after 28 days of exposure to Cu, PP, and combined Cu-PP stress. Combined exposure caused the greatest chlorophyll loss, with total chlorophyll declining to approximately 63.9% of the control level. PP markedly reshaped Cu partitioning: Cu alone was mainly retained in roots, whereas Cu–PP exposure reduced root Cu accumulation but increased leaf Cu content and root-to-leaf translocation. Lignin responses were organ-specific, with enhanced root lignification but reduced leaf lignin accumulation. Multi-omics analyses showed that combined Cu-PP exposure induced a distinct stress state involving chlorophyll/porphyrin metabolism, light-harvesting complexes, phenylpropanoid and flavonoid biosynthesis, redox regulation, hormone signaling, and transport pathways.

Conclusions

PP microplastics reshaped Cu distribution and shifted the primary injury site from roots to leaves, intensifying chloroplast disturbance and defense reprogramming. These findings highlight the need to consider organ-specific metal exposure and multi-omics responses when assessing microplastic–metal co-contamination risks in aquatic plants.

1. Introduction

Freshwater ecosystems are increasingly affected by combined inputs of microplastics, heavy metals, and other contaminants. Wastewater reuse, urban runoff, agricultural discharge, ageing of plastic products, and sediment resuspension promote the long-term coexistence of particulate pollutants and metal ions in aquatic environments [1, 2]. Compared with single-pollutant exposure, combined contamination often produces more complex ecological effects [3, 4]. These effects are influenced not only by the nominal external concentrations of pollutants, but also by particle surface properties, metal speciation, bioavailability, and internal distribution within plants. Therefore, risk assessment of microplastic-metal co-contamination should not rely only on nominal exposure concentrations, but should also consider plant uptake, organ-specific accumulation, and functional injury [5, 6] .

Copper (Cu) is an essential micronutrient involved in photosynthesis, redox regulation, and multiple metalloenzyme-mediated reactions. However, excessive Cu can disrupt nutrient balance, metal homeostasis, and photosynthetic activity, leading to reactive oxygen species accumulation, membrane lipid peroxidation, chlorosis, necrosis, and growth inhibition[7, 8]. Chloroplasts are especially sensitive to Cu overload because chlorophyll metabolism, light-harvesting complex assembly, thylakoid membrane stability, and photosynthetic electron transport require a tightly regulated redox environment [9,–11]. For floating-leaved aquatic plants, the distinction between root retention and leaf redistribution of Cu is therefore central to evaluating toxicity endpoints [12].

The presence of microplastics may further alter Cu migration along the water-root-leaf continuum [13, 14]. Polymer particles can influence the partitioning of metals among dissolved, complexed, and particle-bound forms through adsorption, desorption, surface complexation, oxidative ageing, biofilm formation, and interactions with root exudates [15]. Although polypropylene (PP) is generally characterized by low polarity and hydrophobicity, surface ageing, fragmentation, organic coating, and root-interface retention may still modify Cu contact with root tissues and its subsequent translocation [13]. Thus, combined PP and Cu exposure should be interpreted as an interface-mediated stress scenario rather than a simple sum of two independent stressors [14].

Chlorophyll homeostasis is a key physiological process in plant responses to combined Cu-PP stress. A decline in leaf chlorophyll content may result not only from the classical chlorophyll degradation pathway involving STAY-GREEN (SGR), pheophorbide a oxygenase (PAO), and red chlorophyll catabolite reductase (RCCR), but also from inhibited chlorophyll biosynthesis, abnormal pigment-protein assembly, thylakoid injury, or oxidative pigment depletion[16, 17]. Therefore, pigment reduction should be interpreted together with chloroplast-related genes, photosystem components, and porphyrin/chlorophyll metabolic pathways [16].

Phenylpropanoid metabolism is another important pathway involved in plant responses to metal and microplastic stress. This pathway supplies precursors for lignin, flavonoids, anthocyanins, phenolic acids, and other polyphenolic compounds [18, 19]. Lignin is associated with cell wall reinforcement, apoplastic barrier formation, and metal immobilization, whereas flavonoids and related phenolics contribute to reactive oxygen species scavenging, metal chelation, membrane protection, and photoprotection [18]. Accordingly, changes in carbon allocation between lignin and flavonoid/polyphenol branches may reflect how plants balance structural defense and metabolic detoxification under combined stress [19].

Aquatic macrophytes are major primary producers in shallow-water ecosystems and are widely used in polluted-water remediation and ecological restoration. Floating-leaved plants show clear functional differentiation between roots and leaves: roots directly contact contaminants in water or sediment, whereas leaves mainly perform photosynthesis and gas exchange [20]. This organ-level division makes them useful models for linking contaminant distribution with physiological consequences under combined pollution. Nymphaea 'Black Beauty' is a representative ornamental floating-leaved aquatic

plant, but systematic information remains limited regarding Cu accumulation, PP-mediated exposure shifts, and defense metabolism in water lilies.

Based on this background, the present study used Nymphaea 'Black Beauty' as the experimental material and established a 28-day hydroponic exposure experiment with four treatments: control (CK), Cu exposure alone (CU), PP microplastic exposure alone (PP), and combined Cu-PP exposure (CP). Leaf chlorophyll content, Cu concentrations in roots and leaves, Cu translocation factor, and lignin contents in roots and leaves were measured, and leaf transcriptomics, untargeted metabolomics, and qRT-PCR validation were integrated to examine physiological and molecular responses. This study focused on whether PP alters Cu distribution between roots and leaves, whether leaf Cu accumulation is associated with chlorophyll-homeostasis disruption, whether phenylpropanoid metabolism is redistributed between lignin and flavonoid branches, and whether roots and leaves exhibit distinct defense strategies.

2. Materials and Methods

2.1 Plant material and exposure design

Plants of Nymphaea 'Black Beauty' were obtained from the Xishuangbanna Tropical Botanical Garden, Chinese Academy of Sciences. Healthy plants with uniform morphology, intact leaves, and no visible mechanical damage, pests, or disease symptoms were selected for the experiment, following the general principle that uniform pre-cultivated plant material reduces biological variation in controlled hydroponic assays [21]. Before treatment, all plants were acclimated in half-strength nutrient solution for 14 days under controlled conditions to minimize transplanting effects .

Half-strength Hoagland nutrient solution was used as the basal culture medium to ensure a consistent nutrient supply and ionic background among treatments. Copper sulfate ($CuSO_4$; Shanghai Macklin Biochemical Co., Ltd., China) was used as the Cu source, and the Cu solution was prepared with sterile water and diluted into the culture solution to the target concentration [22]. Polypropylene (PP) microplastics were supplied as 2,000-mesh PP powder; to improve particle dispersion and reduce aggregation, PP powder was mixed with Tween as a dispersing aid, suspended in deionized water, ultrasonicated for 30 min, and then quantitatively added to the nutrient solution [23].

Four treatments were established: CK, half-strength Hoagland nutrient solution as the control; CU, 20 mg L^{-1} Cu; PP, 50 mg L^{-1} PP microplastics; and CP, 20 mg L^{-1} Cu plus 50 mg L^{-1} PP microplastics. Each treatment included three biological replicates, and each replicate contained three plants in an independent container to support biological replication and reduce container-level bias [24]. During the 28-day exposure period, nutrient solutions were renewed weekly to maintain exposure stability and reduce changes caused by nutrient depletion or particle settling.

2.2 Determination of chlorophyll content

At the end of the exposure period, the second fully expanded leaf of each plant was selected for chlorophyll determination. Chlorophyll was extracted using the dimethyl sulfoxide method [25]. Fresh leaf tissue was incubated in dimethyl sulfoxide in the dark, and absorbance was measured at 663 and 645 nm using a UV-visible spectrophotometer (723N). Chlorophyll a, chlorophyll b, and total chlorophyll contents were calculated according to established spectrophotometric equations:

Chl a (mg g-1 FW) = 12.7 x A663–2.69 x A645

Chl b (mg g-1 FW) = 22.9 x A645–4.68 x A663

Total Chl (mg g-1 FW) = Chl a + Chl b

where A663 and A645 represent absorbance values of the extract at 663 and 645 nm, respectively, and FW represents fresh weight [26].

2.3 Determination of Cu content and calculation of translocation factor

After harvest, roots and leaves were separated. Root samples were quickly rinsed with deionized water to remove residual culture solution, attached PP particles, and other surface deposits, and then blotted dry with filter paper [27]. Root and leaf samples were dried at 80 degrees C to constant weight, ground into powder, and passed through a 30–50 mesh sieve to ensure sample homogeneity. Approximately 0.5 g of dried powder was digested with a mixed acid system following microwave/acid digestion principles for plant and siliceous matrices [27], and Cu concentration was determined using inductively coupled plasma mass spectrometry (ICP-MS; Agilent 7700) [28].

The Cu translocation factor (TF) was used to evaluate the relative capacity of Cu transport from roots to leaves, following the common use of organ concentration ratios to assess metal movement in plant exposure studies [28, 29]. It was calculated as follows:

TF = C_leaf / C_root

where C_leaf represents Cu concentration in leaves and C_root represents Cu concentration in roots, both expressed as mg kg-1 DW; a higher TF indicates greater relative transfer of Cu from roots to leaves.

2.4 Determination of lignin content

Root and leaf samples were dried at 80 degrees C to constant weight, ground into homogeneous powder, and sieved. Lignin content was determined using a commercial lignin assay kit (Sangon Biotech, China), with the colorimetric workflow guided by established spectrophotometric principles for lignin quantification [30]. Sample extraction, colorimetric reaction, and measurement were performed according to the manufacturer's protocol, and lignin content was expressed as mg g-1 dry weight.

2.5 RNA sequencing and transcriptomic analysis

Leaf samples from CK, CU, PP, and CP treatments were collected for RNA sequencing, with three biological replicates per treatment. Total RNA was extracted using TRIzol reagent, a phenol/guanidinium-based method widely used for plant RNA isolation, and genomic DNA contamination was removed using DNase I [31]. RNA concentration, purity, integrity, and contamination were assessed using a Qubit fluorometer, NanoDrop spectrophotometer, and Agilent Bioanalyzer, because RNA integrity is a key determinant of sequencing reliability [32].

For each sample, 1 microgram of high-quality RNA was used to construct sequencing libraries. Raw sequencing data were quality-filtered using Trimmomatic v0.36 [33], and clean reads were aligned using HISAT2 [34]. Mapping quality was evaluated using Qualimap v2.2.1 [35], gene-level read counts were generated using featureCounts [36], and differentially expressed genes were identified using edgeR with false discovery rate correction [37–38]. Gene Ontology enrichment was interpreted using the GO framework [39] and GOATOOLS [40], while KEGG pathway analysis was used to identify pathway-level transcriptional changes [41].

2.6 Untargeted metabolomic analysis

Leaf samples from CK, CU, PP, and CP treatments were used for untargeted metabolomic analysis, with three biological replicates per treatment. Samples were ground in liquid nitrogen, extracted with cold methanol/acetonitrile-based solvent, vortexed, ultrasonicated, incubated at low temperature, and centrifuged, consistent with widely used workflows for large-scale plant metabolomic profiling [42]. Quality-control samples were prepared by pooling aliquots from all extracts, and instrumental stability was monitored throughout the run [43]. Raw metabolomic data were processed for peak extraction, alignment, and retention-time correction using XCMS-based principles, and multivariate analyses were used to evaluate treatment-level metabolic separation [44, 45]. Additional multivariate interpretation followed established metabolomics data-analysis principles [46].

2.7 Integrated transcriptomic and metabolomic analysis

To investigate the effects of combined Cu-PP exposure on leaf molecular networks and metabolic outputs at the pathway level, DEGs and differentially accumulated metabolites (DAMs) were jointly mapped to KEGG pathways [41]. The coupling between transcriptional and metabolic changes was evaluated through KEGG enrichment, nine-quadrant analysis, and pathway-level comparison. This integrative strategy follows the logic of multi-omics data analysis, in which transcript and metabolite data are combined to infer pathway-level biological responses [47, 48].

2.8 qRT-PCR validation

To validate the reliability of the transcriptomic results, representative DEGs associated with lignin biosynthesis, flavonoid biosynthesis, light-harvesting complexes, and chlorophyll metabolism were selected for qRT-PCR analysis. Primer design, RNA quality control, and amplification specificity followed the MIQE recommendations for quantitative PCR experiments [49]. Relative expression levels were

calculated using the $2^{-\Delta\Delta Ct}$ method with CK used as the calibrator and an internal reference gene used for normalization [50].

2.9 Statistical analysis

All physiological and biochemical data are presented as the mean +/- standard deviation (SD). Differences among treatments were analyzed using one-way analysis of variance (ANOVA), followed by multiple comparison tests to determine significant differences among treatment means [24]. Statistical significance was accepted at $P < 0.05$. Data visualization was performed using appropriate graphing tools, and transcriptomic/metabolomic multivariate outputs were interpreted in line with established metabolomics and multi-omics analytical principles [45, 48].

3. Results

3.1. Combined Cu–PP exposure aggravated photosynthetic pigment loss in leaves

The treatments significantly altered photosynthetic pigment contents in leaves of Nymphaea 'Black Beauty', but chlorophyll a, chlorophyll b, and total chlorophyll responded differently to single and combined stress. Under CK conditions, Chl a, Chl b, and Total Chl reached 15.80 ± 2.16, 13.88 ± 2.24, and 29.67 ± 4.38 mg g^{-1} FW, respectively. CU treatment did not significantly reduce Chl a but markedly decreased Chl b, suggesting that Cu exposure first disturbed chlorophyll component balance, with the light-harvesting-associated Chl b being more sensitive. PP alone maintained Chl a and Chl b at intermediate levels, indicating a moderate effect on pigment homeostasis. CP treatment caused the strongest pigment decline, reducing Chl a, Chl b, and Total Chl to 10.67 ± 0.40, 8.29 ± 0.88, and 18.96 ± 1.27 mg g^{-1} FW, respectively; Total Chl was only approximately 63.9% of the CK level. Unlike CU, which mainly affected Chl b, CP simultaneously reduced both chlorophyll components and produced the lowest Total Chl value (Fig. 1, Table S1).

3.2. PP altered root-to-leaf Cu partitioning and increased leaf Cu exposure

The treatments significantly changed organ-specific Cu accumulation and root-to-leaf translocation (Fig. 2). Root Cu content remained low under CK and PP treatments, at 13.91 ± 0.55 mg kg^{-1} and a comparable level under PP, indicating that PP alone did not increase root Cu loading. CU treatment strongly increased root Cu to 1062.16 ± 0.79 mg kg^{-1}, approximately 76.34-fold higher than CK, confirming roots as the major Cu-retention site under Cu exposure alone. In contrast, CP sharply reduced root Cu to 121.08 ± 0.18 mg kg^{-1}, corresponding to only 11.40% of the CU level, although still significantly higher than CK and PP. However, this reduction in root Cu was not accompanied by lower leaf Cu. Leaf Cu increased to 126.46 ± 0.32 mg kg^{-1} under CU and further to 149.91 ± 0.29 mg kg^{-1} under CP, approximately 6.73 fold higher than CK. The translocation factor (TF) confirmed that PP reshaped

internal Cu allocation. TF values under CK, PP, and CP were 1.6013 ± 0.1384, 1.2335 ± 0.0643, and 1.2380 ± 0.0024, respectively, whereas CU reduced TF to 0.1191 ± 0.0002 (Table S2). Thus, Cu was largely retained in roots under CU treatment, while PP co-exposure weakened root retention and maintained high leaf Cu exposure.

3.3. Opposite lignin responses in roots and leaves indicate organ-specific structural defense differentiation

Lignin content showed contrasting patterns in leaves and roots, indicating organ-specific defense allocation under Cu–PP co-exposure. Leaf lignin was highest under CK, reaching 144.58 ± 3.93 mg g^{-1}, but decreased to 91.16 ± 0.87 mg g^{-1} under PP. CU and CP further reduced leaf lignin to 58.68 ± 4.51 and 58.24 ± 5.68 mg g^{-1}, respectively, representing decreases of approximately 59% relative to CK (Fig. 2). This pattern suggests that Cu exposure was the main factor suppressing leaf lignin accumulation, and PP co-exposure did not restore lignin deposition. By contrast, root lignin increased under Cu-containing treatments. Compared with CK at 61.73 ± 5.10 mg g^{-1}, root lignin increased slightly under PP, rose to 93.77 ± 5.24 mg g^{-1} under CU, and reached 128.27 ± 6.26 mg g^{-1} under CP, approximately 107.79% higher than CK, (Table S3).

3.4. Transcriptome wide variation, differential expression patterns, and functional enrichment

Principal component analysis showed clear transcriptomic separation among CK, CU, PP, and CP treatments, with close clustering of biological replicates. PC1 and PC2 explained 46.54% and 19.21% of the total variance, respectively. CK and CU were mainly positioned on the negative side of PC1, whereas PP and CP shifted to the positive side, indicating that PP exposure, alone or with Cu, was a major driver of leaf transcriptional remodeling (Fig. 3A,Table S4). The sample correlation heatmap further confirmed replicate reliability and treatment-specific expression patterns.

Using $|\log_2 FC| > 2$ and FDR < 0.05 as thresholds, the largest DEG numbers were detected in CU vs CP and CK vs CP, with approximately 4.17×10^3 and 3.81×10^3 DEGs, respectively. This indicates that CP differed markedly from both the control and Cu exposure alone. CK vs PP and CK vs CU contained approximately $2.70 \times 10^3$and 1.80×10^3 DEGs, while PP vs CP contained approximately 1.40×10^3 DEGs, showing that Cu addition under PP exposure still induced specific transcriptional reprogramming (Fig. 3B-D,Table S5). Venn analysis identified 145 shared DEGs across the five comparisons, together with many treatment-specific DEGs, supporting the interpretation that CP represented an independent combined-stress expression state rather than a simple sum of CU and PP responses.

KEGG enrichment showed that DEGs were mainly associated with primary and secondary metabolism, signal transduction, antioxidant defense, and membrane transport. Enriched pathways included metabolic pathways, biosynthesis of secondary metabolites, phenylpropanoid and flavonoid biosynthesis, glutathione and sulfur metabolism, plant hormone signaling, MAPK signaling, ABC

transporters, starch and sucrose metabolism, fatty acid elongation, and cutin, suberine, and wax biosynthesis. These results indicate that Cu, PP, and CP simultaneously affected redox buffering, transport, carbohydrate allocation, cell-wall/cuticle processes, and secondary defense metabolism (Fig. 3E-F).

3.5. Untargeted metabolomic analysis

Untargeted metabolomic PCA separated CK, CU, PP, and CP treatments, with biological replicates clustering within each group. PC1 and PC2 explained 40.08% and 22.20% of the total metabolic variance, respectively, indicating that single and combined exposures all altered the leaf metabolic state, with CP forming a distinct metabolic profile. Chemical classification showed that differentially accumulated metabolites (DAMs) were mainly lipids and lipid-like molecules, organic acids and derivatives, organic heterocyclic compounds, and phenylpropanoids/polyketides. Lipids accounted for approximately 30% of DAMs, while organic acids and heterocyclic compounds each accounted for approximately 15%, and phenylpropanoids/polyketides for approximately 13% (Fig. 4A-C,,Table S6).

Across comparisons, 1,831, 1,799, and 1,717 DAMs were detected in CK vs CU, CK vs CP, and CK vs PP, respectively, while 1,496 and 1,450 DAMs were detected in CP vs CU and CP vs PP. These results indicate that CP remained metabolically distinct from either single treatment. Venn analysis identified 406 DAMs shared across all comparisons, together with comparison-specific metabolites. Key DAMs included phenolic acids, polyphenols, flavonoids and their glycosylated or acylated derivatives, and several lipophilic or resin-acid-like compounds, such as gallic acid, dehydroabietic acid, acetylsalicylic acid, quercetin derivatives, orientin, eriodictyol, delphinidin, and leonurine (Fig. 4D-F,Table S7).

3.6. Integrated transcriptomic and metabolomic analysis

To clarify the relationship between transcriptional and metabolic changes, DEGs and DAMs were analyzed using nine-quadrant distribution, KEGG up and down regulation statistics, and joint enrichment analysis. The nine-quadrant plot showed no simple global one to one correspondence between DEGs and DAMs. Most gene metabolite pairs were located in quadrant 5, indicating no simultaneous significant change under the defined thresholds. Quadrants 2 and 8 contained many pairs in which metabolites changed significantly while related genes did not, suggesting partial uncoupling between transcript abundance and metabolite accumulation. This pattern is consistent with the complexity of metabolic regulation, which may also depend on enzyme activity, substrate availability, transport, feedback regulation, metabolite modification, and temporal delays. Therefore, pathway-level convergence is more informative than individual gene–metabolite correlations under Cu–PP co-exposure (Fig. 5,Table S8).

Despite this partial uncoupling, integrated pathway analysis revealed coordinated functional changes. DEGs and DAMs were jointly mapped to porphyrin metabolism, phenylpropanoid biosynthesis, flavonoid biosynthesis, starch and sucrose metabolism, plant hormone signal transduction, alpha-linolenic acid

metabolism, ascorbate and aldarate metabolism, and amino sugar and nucleotide sugar metabolism. These pathways correspond to chlorophyll metabolism, phenylpropanoid flavonoid defense, carbohydrate allocation, hormone and lipid-derived signaling, and antioxidant metabolism. The enrichment of porphyrin metabolism was consistent with the marked chlorophyll decline under CP, whereas phenylpropanoid and flavonoid pathways corresponded to reduced leaf lignin and increased polyphenol/flavonoid metabolites.

3.7. Key pathway mapping reveals chloroplast disturbance and defensive carbon redistribution

To link high leaf Cu loading, chlorophyll loss, and defense remodeling, DEGs and DAMs were mapped to light-harvesting complex, porphyrin/chlorophyll metabolism, phenylpropanoid metabolism, and flavonoid biosynthesis pathways. Compared with CK, PP and especially CP generally induced PSI and PSII light-harvesting complex genes, including *Lhca1–Lhca5* and *Lhcb1–Lhcb7.* Because this induction occurred together with the lowest Total Chl content under CP, it likely reflects compensatory transcriptional regulation under pigment loss and photosystem stress rather than improved photosynthetic capacity.

Porphyrin and chlorophyll metabolism showed asynchronous regulation of biosynthesis, assembly, and degradation. Biosynthetic or precursor-conversion genes, including *CHLH, CHLI, CHLM, CHL27, POR*, and *DVR*, were induced to varying degrees under PP or CP. In contrast, *PAO* and *RCCR* tended to be downregulated, and red chlorophyll catabolite abundance decreased accordingly, while SGR showed inconsistent changes. Thus, chlorophyll loss under CP was unlikely to result from broad activation of the canonical SGR-PAO/RCCR degradation pathway; instead, it likely reflected an imbalance among chlorophyll biosynthesis, pigment–protein assembly, pigment stability, and oxidative loss (Fig. 6).

Phenylpropanoid metabolism was also reconfigured. Genes associated with lignin monomer biosynthesis, including *CYP73A/C4H, 4CL1, C3H, CCR1, COMT*, and related methyltransferases, were generally downregulated or inconsistently expressed under PP and CP. Conversely, flavonoid pathway genes, including CHS, *CHI, F3H, F3’H, F3’5’H, DFR*, and *LDOX/ANS*, were maintained at higher levels or upregulated, accompanied by increased flavonoid and anthocyanin related metabolites such as eriodictyol and delphinidin, particularly under CP. Together with decreased leaf lignin and increased root lignin, these pathway-level results suggest that phenylpropanoid carbon flux was redistributed rather than globally enhanced under Cu-PP co-exposure. Roots favored lignification-based structural defense, whereas leaves shifted from lignin deposition toward soluble chemical defense involving flavonoids, anthocyanins, and polyphenols.

3.8. qRT-PCR validation of key pathway-related genes

Seven candidate genes related to lignin biosynthesis, flavonoid biosynthesis, light-harvesting complexes, and chlorophyll metabolism were selected for qRT-PCR validation. In the lignin branch of phenylpropanoid metabolism, CCR and *4CL1* were progressively downregulated and reached their lowest

expression under CP, confirming suppression of leaf lignin biosynthesis at the transcriptional level. By contrast, the flavonoid biosynthesis gene *F3H* was induced under CU and PP and peaked under CP, at approximately threefold the CK level, supporting a shift toward flavonoid based soluble defense (Fig. 7,Table S9). The light harvesting complex genes *Lhca4* and *Lhcb6* were significantly upregulated under CP, with *Lhcb6* reaching approximately fivefold the CK level, further supporting compensatory induction of LHC-family genes under combined stress. Chlorophyll metabolism-related genes showed branch-specific regulation: Nyc1 was significantly downregulated under PP and CP, whereas *CHL27* remained relatively highly expressed in Cu-containing treatments

4. Discussion

4.1. PP altered Cu distribution along the root-leaf axis and shifted the primary stressed organ to leaves

A key finding of this study is that PP microplastics did not simply intensify or alleviate Cu toxicity, but markedly reshaped Cu distribution in Nymphaea 'Black Beauty'. Under Cu exposure alone, Cu was predominantly retained in roots, whereas combined Cu-PP exposure reduced root Cu accumulation but increased leaf Cu content and restored the translocation factor toward a higher level [51, 52]. Similar combined-contamination studies have shown that micro- or nanoplastics can modify metal uptake, translocation, and toxicity rather than acting as inert background particles [51, 53].

This redistribution suggests that the risk of combined contamination cannot be evaluated solely by external Cu concentration or root metal accumulation [54, 55]. In floating-leaved aquatic plants, leaves are the main organs responsible for photosynthetic carbon assimilation, so enhanced leaf Cu loading may shift the dominant injury endpoint from root retention toward leaf chloroplast dysfunction [56]. Studies on PP microplastics and nanoplastics also show that plastic particles can reshape plant metabolic pathways, photosynthesis, and defense outputs in a size-, dose-, and tissue-dependent manner [54, 56]. Non-targeted metallomics and deep-learning screening further emphasize that micro/nanoplastic phytotoxicity can involve altered metal distributions and leaf-level physiological injury. The effects of PP alone also appear context-dependent. In some systems, plastic particles mainly induce oxidative stress, photosynthetic inhibition, and root architectural disruption, whereas remediation or buffering effects depend on species traits, particle properties, and exposure routes [57]. In the present study, PP alone caused limited Cu accumulation but did not fully reproduce the CP phenotype, indicating that the combined response depended on the interaction between PP-mediated interface effects and Cu availability rather than on PP exposure alone [58].

4.2. High leaf Cu exposure disrupted chloroplast homeostasis rather than simply enhancing chlorophyll degradation

In the CP treatment, the highest leaf Cu content coincided with the most pronounced loss of photosynthetic pigments. Chl a, Chl b, and total chlorophyll decreased strongly under combined

exposure, suggesting that enhanced leaf Cu pressure directly affected pigment homeostasis. Studies of CuO nanoparticles and ionic/bulk Cu in plants demonstrate that excessive Cu can induce oxidative stress, nutrient imbalance, hormonal disturbance, and photosynthetic impairment [59, 60]. This pattern also agrees with broader evidence that nanoparticles and microplastic particles can influence plant transport, toxicity, and chloroplast-related physiology The net chlorophyll loss under CP treatment was more likely associated with broader disruption of chloroplast homeostasis than with simple activation of chlorophyll degradation [55, 61]. In tomato seedlings, microplastic exposure inhibited photosynthetic pigment synthesis by down-regulating key genes in chlorophyll and heme pathways and reducing pigment precursors [55]. In ornamental tulip, copper nanoparticles affected chlorophyll maintenance, membrane stability, and antioxidant enzymes, further indicating that Cu-containing particles or Cu exposure can influence pigment status through multiple physiological routes [61].

This interpretation is consistent with studies showing that plant growth inhibition under plastic particle stress is usually accompanied by coordinated changes in photosynthesis, redox regulation, ion homeostasis, hormone signaling, and immunity-related pathways [56, 62]. Polyethylene nanoplastics, for example, can rapidly induce stomatal closure, ROS accumulation, and defense gene activation in tobacco leaves. Therefore, the CP treatment in Nymphaea should be viewed as a chloroplast-centered and defense-linked response state, not only as a pigment-degradation phenotype [62].

4.3. Phenylpropanoid-derived defenses were redistributed between root structural barriers and leaf chemical protection

Combined Cu-PP stress markedly reshaped the organ-specific allocation of phenylpropanoid-derived defenses. Leaf lignin content decreased under Cu and CP treatments, whereas root lignin increased most strongly under CP, suggesting that roots reinforced structural barriers while leaves redirected carbon away from lignin deposition. PP-MP exposure in tobacco leaves similarly altered phenylpropanoid and flavonoid biosynthesis, lignin-related genes, and lignin-degrading enzymes, supporting the sensitivity of this pathway to PP-MP stress [63]. Recent work on PP microplastics and cadmium co-pollution in wheat-soil systems further supports the need to interpret PP-metal co-exposure from multiple physiological and molecular perspectives. This redistribution has physiological relevance. Lignin is a carbon-intensive and relatively slow-forming structural defense that reinforces cell walls and supports long-term barrier formation, whereas flavonoids, polyphenols, and antioxidant metabolites can respond more rapidly to oxidative stress and metal pressure [64]. Studies on microplastic-metal interactions also suggest that plant metal uptake and toxicity are closely linked to particle-mediated changes in bioavailability and internal distribution [65].

Evidence from studies on plant metal exposure and microplastic-associated stress supports this interpretation. Polystyrene nanoplastics can distinctly affect cadmium uptake and toxicity in Arabidopsis, while microplastics can alter heavy-metal bioaccumulation in Brassica napus, indicating that plastic particles may reshape both metal transport and downstream defense metabolism [66, 67]. In

Nymphaea, the coexistence of enhanced root lignin and reduced leaf lignin therefore suggests a division of labor between root structural immobilization and leaf metabolic protection [64].

4.4. Multi-omics evidence indicates that CP represents an independent combined-stress state rather than an additive Cu-PP response

Transcriptomic and metabolomic analyses indicated that the CP response was not a linear combination of the Cu and PP responses. Meta-analytic and rhizosphere studies show that the impacts of microplastics on plant metal accumulation, enzyme activity, soil-rhizosphere processes, and microbial communities vary markedly with polymer type, size, exposure concentration, and coexisting metals [68, 69]. The separation of CP samples in PCA and the large number of DEGs and DAMs therefore support the interpretation that combined Cu-PP exposure represents an independent stress state. Previous studies under Cd, Pb, or other metal contamination have shown that microplastics and nanoplastics can modify plant photosynthesis, root growth, oxidative stress, hormone signaling, and nutrient uptake [70, 71]. In contrast, the present hydroponic system minimized soil-mediated pathways and highlighted the water-root-leaf interface as a key exposure route. The observed increase in leaf Cu under CP suggests that PP-mediated interfacial processes can alter internal metal allocation even in the absence of complex soil matrices [70]. Hydroponic studies of rice seedlings also demonstrate that nano/microplastics can be taken up and translocated within plant tissues, providing a mechanistic basis for internal exposure shifts.

Overall, the results support a mechanistic sequence in which PP first altered Cu distribution along the root-leaf axis, shifting exposure from strong root retention toward increased leaf accumulation [72, 73]. Elevated leaf Cu then disrupted chloroplast homeostasis, photosynthetic pigment maintenance, redox balance, and energy metabolism [74, 75]. In parallel, phenylpropanoid metabolism was redistributed between root lignin reinforcement and leaf flavonoid/polyphenol-related protection [76, 77]. These responses ultimately generated a CP-specific molecular and physiological state, emphasizing the need to integrate exposure interface, metal partitioning, organ specificity, and multi-omics evidence when assessing microplastic-metal risks in aquatic plants [78, 79]. Comparable Cu-localization and subcellular-distribution studies in aquatic and woody plants indicate that Cu toxicity is strongly determined by tissue localization, chemical form, and compartmentation rather than by total exposure alone [80, 81]. Flavonoid biosynthesis and phenolic metabolism are also central components of stress adaptation, metal chelation, and antioxidant protection [86, 87]. Finally, strong expression differences in metal homeostasis and lignin-related genes between metal-adapted and non-adapted plants support the relevance of cell-wall and phenylpropanoid pathways in metal-stress tolerance [82].

5. Conclusion

This study demonstrates that PP microplastics fundamentally altered Cu toxicity in Nymphaea ‘Black Beauty’ by redistributing Cu along the root-leaf axis. Under Cu exposure alone, Cu was largely retained in roots; however, combined Cu-PP exposure reduced root Cu accumulation while increasing leaf Cu

exposure, thereby aggravating photosynthetic pigment loss. The molecular and metabolic responses further indicated that combined Cu-PP stress was not a simple additive effect of the two pollutants, but an independent combined-stress state involving chloroplast homeostasis disruption, redox adjustment, transport regulation, and secondary metabolic reprogramming. A key mechanism revealed by this study is the organ-specific redistribution of phenylpropanoid derived defenses. Roots enhanced lignification, suggesting structural reinforcement and potential apoplastic barrier formation, whereas leaves showed reduced lignin accumulation and increased flavonoid, anthocyanin, and polyphenol related responses. These findings suggest that PP-mediated Cu redistribution can shift the functional burden of toxicity from belowground retention to aboveground photosynthetic injury. Therefore, ecological risk assessment of microplastic metal co-contamination should consider not only total metal accumulation, but also organ-level exposure, pigment damage, defense allocation, and integrated molecular responses.

Declarations

Acknowledgments

Not applicable.

Author contributions

Yuhong Rong: Investigation, Writing -original draft, Validation, Data curation, Software, Conceptualization. **Hongjun Mu**: Project administration, Investigation, Validation. **Ziyu Li:** Data curation,Validation. **Zhaohao Zhang:** Investigation,Data curation. **Jiang Xie:** Investigation. **Yongbo Zhang:**Investigation. **Yanyin Xu:** Data curation. **Shen Xiong:** Data curation. **Zesen Lai:** Data curation. **Haiying Xiong:** Resources. **Kaixiong Li:** Investigation. **Shanman Li:** Data curation. **Chao Luo:** Writing - review & editing, Supervision, Conceptualization, Project administration.

Funding

This work was supported by the Yunnan Provincial Agricultural Joint Special Project ("Genetic Diversity Analysis and Conservation Techniques of Water Lily (Nymphaea) Germplasm Resources", 202301BD070001-259); Special Project for the Construction of the Tropical Crop Science and Technology Innovation System in Yunnan Province ("Development and Utilization of ‘High-yielding, Novel, Exotic, Unique, and Superior’ Tropical Crop Germplasm Resources", RF2026-19); Special Project for the Construction of the Tropical Crop Science and Technology Innovation System in Yunnan Province ("Soil Remediation of Glyphosate Contamination and Its Impact on the Rhizosphere Microenvironment in Young Rubber Tree/Leguminous Green Manure Intercropping Systems", QNCZ2025-9).the Guizhou University Talent Introduction Research Project: Systematic Evolution and Genetic Diversity of Wild Impatiens in Guizhou (X2023091); Molecular Mechanism of Phylogenetic Development of Wild Impatiens in Karst Regions (X2023331); Study on the Molecular Mechanism of Jasmine Flower Scent Synthesis (Z2024667)

Data availability Statement

he raw RNA-seq reads generated in this study have been submitted to the Genome Sequence Archive (GSA), National Genomics Data Center, China National Center for Bioinformation / Beijing Institute of Genomics, Chinese Academy of Sciences, under the submission ID subCRA073211. The final GSA accession number will be provided once assigned by the repository. Processed transcriptomic data, including gene-count matrices and DEG lists, together with metabolomics feature tables, metabolite annotation tables, DAM lists, qRT-PCR data, and supporting physiological and biochemical datasets, are available in the Supplementary Materials.

Ethics approval and consent to participate

Not applicable

Consent for publication

Not applicable

Competing interests

The authors declare no competing interests

Author details

1:Yunnan Institute of Tropical Crops, Jinghong 666100, China;

2:College of Life Science, Guizhou University, Guiyang, 550025, China;

References

1. Geyer R, Jambeck JR, Law KL. Production, use, and fate of all plastics ever made. Sci Adv. 2017;3:e1700782.
2. PlasticsEurope. Plastics - the Facts 2024: an analysis of European plastics production, demand and waste data. Brussels: PlasticsEurope; 2024. Available from: https://plasticseurope.org/knowledge-hub/plastics-the-facts-2024/
3. Tursi A, Baratta M, Easton T, Chatzisymeon E, Chidichimo F, De Biase M, et al. Microplastics in aquatic systems, a comprehensive review: origination, accumulation, impact, and removal technologies. RSC Adv. 2022;12:28318–40.
4. Ge J, Li H, Liu P, Zhang Z, Ouyang Z, Guo X. Review of the toxic effect of microplastics on terrestrial and aquatic plants. Sci Total Environ. 2021;791:148333.
5. Tariq M, Iqbal B, Khan I, Khan AR, Jho EH, Salam A, et al. Microplastic contamination in the agricultural soil-mitigation strategies, heavy metals contamination, and impact on human health: a review. Plant Cell Rep. 2024;43:1–15.

6. Khan AR, Ulhassan Z, Li G, Lou J, Iqbal B, Salam A, et al. Micro/nanoplastics: critical review of their impacts on plants, interactions with other contaminants, and management strategies. Sci Total Environ. 2024;912:169477.
7. Khalid N, Aqeel M, Noman A, Khan SM, Akhter N. Interactions and effects of microplastics with heavy metals in aquatic and terrestrial environments. Environ Pollut. 2021;290:118104.
8. Cao Y, Zhao M, Ma X, Song Y, Zuo S, Li H, et al. A critical review on the interactions of microplastics with heavy metals: mechanism and their combined effect on organisms and humans. Sci Total Environ. 2021;788:147620.
9. Yruela I. Copper in plants: acquisition, transport and interactions. Funct Plant Biol. 2009;36:409–30.
10. Mir AR, Pichtel J, Hayat S. Copper: uptake, toxicity and tolerance in plants and management of Cu-contaminated soil. Biometals. 2021;34:737–59.
11. Wu J, Wang T, Huang Y, Xiao S, Luo X, Deng Y, et al. Genotypic difference in response to copper stress in upland cotton as revealed by physiological and molecular expression analyses. BMC Plant Biol. 2025;25:21.
12. Abbasirad S, Ghotbi-Ravandi AA. Toxicity of copper oxide nanoparticles in barley: induction of oxidative stress, hormonal imbalance, and systemic resistances. BMC Plant Biol. 2025;25:187.
13. Roy R, Hossain A, Sultana S, Deb B, Ahmod MM, Sarker T. Microplastics increase cadmium absorption and impair nutrient uptake and growth in red amaranth (Amaranthus tricolor L.) in the presence of cadmium and biochar. BMC Plant Biol. 2024;24:608.
14. Noor MA, Huang G, Chattha MB, Zhou B, Hassan MU, Al-Khayri JM, et al. Silicon mitigates combined cadmium and microplastics toxicity in rice by regulating glyoxalase system, and phytochelatin-mediated cadmium detoxification. BMC Plant Biol. 2026;26:744.
15. Li M, Liu Y, Xu G, Wang Y, Yu Y. Impacts of polyethylene microplastics on bioavailability and toxicity of metals in soil. Sci Total Environ. 2021;760:144037.
16. El-Mahdy MT, Abulfadl EA, Dawood MFA. Aluminum and copper oxide nanoparticles alter secondary metabolites, antioxidants, and biochemical markers in key lime: in vitro approach. BMC Plant Biol. 2026;26:98.
17. Liu H, Tang H, Gao Y, An Y, Zhou J, Li X, et al. The multifaceted mechanisms of microplastic inhibition of tomato plant growth: oxidative toxicity, metabolic perturbation, and photosynthetic damage. Plant Physiol Biochem. 2026;230:110976.
18. Arshad M, Ma Y, Gao W, Zhang S, Shoaib M, Liu X, et al. Polypropylene microplastic exposure modulates multiple metabolic pathways in tobacco leaves, impacting lignin biosynthesis. Ecotoxicol Environ Saf. 2025;292:118005.
19. Bonawitz ND, Chapple C. The genetics of lignin biosynthesis: connecting genotype to phenotype. Annu Rev Genet. 2010;44:337–63.
20. Lacoul P, Freedman B. Environmental influences on aquatic plants in freshwater ecosystems. Environ Rev. 2006;14:89–136.

21. Hoagland DR, Arnon DI. The water-culture method for growing plants without soil. Berkeley: California Agricultural Experiment Station; 1950.
22. Zong X, Zhang J, Zhu J, Zhang L, Jiang L, Yin Y, et al. Effects of polystyrene microplastic on uptake and toxicity of copper and cadmium in hydroponic wheat seedlings (Triticum aestivum L). Ecotoxicol Environ Saf. 2021;217:112217.
23. Shorobi FM, Vyavahare GD, Seok YJ, Park JH. Effect of polypropylene microplastics on seed germination and nutrient uptake of tomato and cherry tomato plants. Chemosphere. 2023;329:138679.
24. Quinn GP, Keough MJ. Experimental design and data analysis for biologists. Cambridge: Cambridge University Press; 2002.
25. Hiscox JD, Israelstam GF. A method for the extraction of chlorophyll from leaf tissue without maceration. Can J Bot. 1979;57:1332–4.
26. Arnon DI. Copper enzymes in isolated chloroplasts: polyphenoloxidase in Beta vulgaris. Plant Physiol. 1949;24:1–15.
27. United States Environmental Protection Agency. Method 3052: microwave assisted acid digestion of siliceous and organically based matrices. Washington, DC: US Environmental Protection Agency; 1996.
28. Mwamba TM, Li L, Gill RA, Islam F, Nawaz A, Ali B, et al. Differential subcellular distribution and chemical forms of cadmium and copper in Brassica napus. Environ Exp Bot. 2016;134:239–49.
29. Liu Y, Guo R, Zhang S, Sun Y, Wang F. Uptake and translocation of nano/microplastics by rice seedlings: evidence from a hydroponic experiment. J Hazard Mater. 2021;403:123997.
30. Fukushima RS, Hatfield RD. Comparison of the acetyl bromide spectrophotometric method with other analytical lignin methods. J Agric Food Chem. 2004;52:3713–20.
31. Chomczynski P, Sacchi N. Single-step method of RNA isolation by acid guanidinium thiocyanate-phenol-chloroform extraction. Anal Biochem. 1987;162:156–9.
32. Schroeder A, Mueller O, Stocker S, Salowsky R, Leiber M, Gassmann M, et al. The RIN: an RNA integrity number for assigning integrity values to RNA measurements. BMC Mol Biol. 2006;7:3.
33. Bolger AM, Lohse M, Usadel B. Trimmomatic: a flexible trimmer for Illumina sequence data. Bioinformatics. 2014;30:2114–20.
34. Kim D, Paggi JM, Park C, Bennett C, Salzberg SL. Graph-based genome alignment and genotyping with HISAT2 and HISAT-genotype. Nat Biotechnol. 2019;37:907–15.
35. Okonechnikov K, Conesa A, Garcia-Alcalde F. Qualimap 2: advanced multi-sample quality control for high-throughput sequencing data. Bioinformatics. 2016;32:292–4.
36. Liao Y, Smyth GK, Shi W. featureCounts: an efficient general-purpose program for assigning sequence reads to genomic features. Bioinformatics. 2014;30:923–30.
37. Robinson MD, McCarthy DJ, Smyth GK. edgeR: a Bioconductor package for differential expression analysis of digital gene expression data. Bioinformatics. 2010;26:139–40.

38. Benjamini Y, Hochberg Y. Controlling the false discovery rate: a practical and powerful approach to multiple testing. J R Stat Soc Ser B Methodol. 1995;57:289–300.
39. Ashburner M, Ball CA, Blake JA, Botstein D, Butler H, Cherry JM, et al. Gene Ontology: tool for the unification of biology. Nat Genet. 2000;25:25–9.
40. Klopfenstein DV, Zhang L, Pedersen BS, Ramirez F, Warwick Vesztrocy A, Naldi A, et al. GOATOOLS: a Python library for Gene Ontology analyses. Sci Rep. 2018;8:10872.
41. Kanehisa M, Goto S. KEGG: Kyoto Encyclopedia of Genes and Genomes. Nucleic Acids Res. 2000;28:27–30.
42. Dunn WB, Broadhurst D, Begley P, Zelena E, Francis-McIntyre S, Anderson N, et al. Procedures for large-scale metabolic profiling of serum and plasma using gas chromatography and liquid chromatography coupled to mass spectrometry. Nat Protoc. 2011;6:1060–83.
43. Smith CA, Want EJ, O'Maille G, Abagyan R, Siuzdak G. XCMS: processing mass spectrometry data for metabolite profiling using nonlinear peak alignment, matching, and identification. Anal Chem. 2006;78:779–87.
44. Patti GJ, Yanes O, Siuzdak G. Metabolomics: the apogee of the omics trilogy. Nat Rev Mol Cell Biol. 2012;13:263–9.
45. Fiehn O. Metabolomics-the link between genotypes and phenotypes. Plant Mol Biol. 2002;48:155–71.
46. Worley B, Powers R. Multivariate analysis in metabolomics. Curr Metabolomics. 2013;1:92–107.
47. Chong J, Wishart DS, Xia J. Using MetaboAnalyst 4.0 for comprehensive and integrative metabolomics data analysis. Curr Protoc Bioinf. 2019;68:e86.
48. Rohart F, Gautier B, Singh A, Le Cao KA. mixOmics: an R package for omics feature selection and multiple data integration. PLoS Comput Biol. 2017;13:e1005752.
49. Bustin SA, Benes V, Garson JA, Hellemans J, Huggett J, Kubista M, et al. The MIQE guidelines: minimum information for publication of quantitative real-time PCR experiments. Clin Chem. 2009;55:611–22.
50. Livak KJ, Schmittgen TD. Analysis of relative gene expression data using real-time quantitative PCR and the 2-DeltaDeltaCT method. Methods. 2001;25:402–8.
51. Peng J, Yan Q, Hassan MU, Imran M, Haider FU, Liang J, et al. Metarhizium anisopliae mitigates the phytotoxicity of lead and nanoplastics on rice by modifying physiological, transcriptomic, metabolomic activities, and soil microbiome. Adv Sci. 2026;13:e21570.
52. Noor MA, Huang G, Chattha MB, Zhou B, Hassan MU, Al-Khayri JM, et al. Silicon mitigates combined cadmium and microplastics toxicity in rice by regulating glyoxalase system, and phytochelatin-mediated cadmium detoxification. BMC Plant Biol. 2026;26:744.
53. Roy R, Hossain A, Sultana S, Deb B, Ahmod MM, Sarker T. Microplastics increase cadmium absorption and impair nutrient uptake and growth in red amaranth (Amaranthus tricolor L.) in the presence of cadmium and biochar. BMC Plant Biol. 2024;24:608.

54. Arshad M, Ma Y, Gao W, Zhang S, Shoaib M, Liu X, et al. Polypropylene microplastic exposure modulates multiple metabolic pathways in tobacco leaves, impacting lignin biosynthesis. Ecotoxicol Environ Saf. 2025;292:118005.
55. Liu H, Tang H, Gao Y, An Y, Zhou J, Li X, et al. The multifaceted mechanisms of microplastic inhibition of tomato plant growth: oxidative toxicity, metabolic perturbation, and photosynthetic damage. Plant Physiol Biochem. 2026;230:110976.
56. Liu X, Zhang H, Su T, Arshad M, Gao W, Zhang S, et al. Multi-omics analysis reveals immune responses in tobacco leaves treated with polyethylene nanoparticles. Plant Physiol Biochem. 2026;231:111026.
57. Feng Y, Zhao E, Yan B, Wang B, Liang H, Fan S, Gu X. Root architecture-informed nano-remediation strategy for nanoplastics toxicity in maize and soybean. Plant Physiol Biochem. 2026;230:110756.
58. El-Mahdy MT, Abulfadl EA, Dawood MFA. Aluminum and copper oxide nanoparticles alter secondary metabolites, antioxidants, and biochemical markers in key lime: in vitro approach. BMC Plant Biol. 2026;26:98.
59. Abbasirad S, Ghotbi-Ravandi AA. Toxicity of copper oxide nanoparticles in barley: induction of oxidative stress, hormonal imbalance, and systemic resistances. BMC Plant Biol. 2025;25:187.
60. Wu J, Wang T, Huang Y, Xiao S, Luo X, Deng Y, et al. Genotypic difference in response to copper stress in upland cotton as revealed by physiological and molecular expression analyses. BMC Plant Biol. 2025;25:21.
61. Abbas N, Ahmed S, Ansari M, Alamri S, Alfagham AT. Phytogenic synthesis of copper nanoparticles by using leaf extract of Eucalyptus globulus and its antifungal activity against Fusarium oxysporum and Fusarium solani. BMC Plant Biol. 2025;25:1519.
62. El-Sayed IM, El-Ziat RA, Othman EZ. Chitosan and copper nanoparticles in vase solutions elevate the quality and longevity of cut tulips, setting a new standard for sustainability in floriculture. BMC Plant Biol. 2025;25:780.
63. Abbasi S, Moore F, Keshavarzi B, Hopke PK, Naidu R, Rahman MM, et al. PET-microplastics as a vector for heavy metals in a simulated plant rhizosphere zone. Sci Total Environ. 2020;744:140984.
64. Zong X, Zhang J, Zhu J, Zhang L, Jiang L, Yin Y, et al. Effects of polystyrene microplastic on uptake and toxicity of copper and cadmium in hydroponic wheat seedlings (Triticum aestivum L). Ecotoxicol Environ Saf. 2021;217:112217.
65. Xu G, Lin X, Yu Y. Different effects and mechanisms of polystyrene micro- and nano-plastics on the uptake of heavy metals (Cu, Zn, Pb and Cd) by lettuce (Lactuca sativa L). Environ Pollut. 2023;316:120656.
66. Li J, Zhang Y, Zhou Y, Liu W, Maryam B, Cui J, et al. Polystyrene nanoplastics distinctly impact cadmium uptake and toxicity in Arabidopsis thaliana. Environ Pollut. 2024;356:124373.
67. Jia H, Wu D, Yu Y, Han S, Sun L, Li M. Impact of microplastics on bioaccumulation of heavy metals in rape (Brassica napus L). Chemosphere. 2022;288:132576.

68. Chen L, Chang N, Qiu T, Wang N, Cui Q, Zhao S, Huang F, et al. Meta-analysis of impacts of microplastics on plant heavy metal(loid) accumulation. Environ Pollut. 2024;348:123787.
69. Lian Y, Shi R, Liu J, Zeb A, Wang Q, Wang J, Yu M, et al. Effects of polystyrene, polyethylene, and polypropylene microplastics on the soil-rhizosphere-plant system: phytotoxicity, enzyme activity, and microbial community. J Hazard Mater. 2024;465:133417.
70. Shorobi FM, Vyavahare GD, Seok YJ, Park JH. Effect of polypropylene microplastics on seed germination and nutrient uptake of tomato and cherry tomato plants. Chemosphere. 2023;329:138679.
71. Ren X, Tang J, Wang L, Liu Q. Microplastics in soil-plant system: effects of nano/microplastics on plant photosynthesis, rhizosphere microbes and soil properties in soil with different residues. Plant Soil. 2021;462:561–76.
72. Yu Y, Li J, Song Y, Zhang Z, Yu S, Xu M, Zhao Y. Stimulation versus inhibition: the effect of microplastics on pak choi growth. Appl Soil Ecol. 2021;177:104505.
73. Bosker T, Bouwman LJ, Brun NR, Behrens P, Vijver MG. Microplastics accumulate on pores in seed capsule and delay germination and root growth of the terrestrial vascular plant Lepidium sativum. Chemosphere. 2019;226:774–81.
74. Liu Y, Xu F, Ding L, Zhang G, Bai B, Han Y, Xiao L, et al. Microplastics reduce nitrogen uptake in peanut plants by damaging root cells and impairing soil nitrogen cycling. J Hazard Mater. 2023;443:130384.
75. Li H, Song F, Song X, Zhu K, Lin Q, Zhang J, Ning G. Single and composite damage mechanisms of soil polyethylene/polyvinyl chloride microplastics to the photosynthetic performance of soybean (Glycine max [L.] Merr). Front Plant Sci. 2023;13:1100291.
76. Nuamzanei CU, Sk S, Kumar N, Borah B, Chikkaputtaiah C, Saikia R, Phukan T. Impact of polyvinyl chloride microplastic on growth, photosynthesis and nutrient uptake of Solanum lycopersicum L. Environ Pollut. 2024;349:123994.
77. Zhang Z, Zhao L, Jin Q, Luo Q, He H. Combined contamination of microplastic and antibiotic alters the composition of microbial community and metabolism in wheat and maize rhizosphere soil. J Hazard Mater. 2024;473:134618.
78. Zhao S, Zhang Q, Chen X, Huang Q, Li H, Siddique KHM. Biochar counteracts the negative effects of microplastics on physiological and biochemical characteristics and leaf metabolism in Zea mays L. J Hazard Mater. 2025;496:139355.
79. Wu C, Ma Y, Wang D, Shan Y, Song X, Hu H, Ma Y. Integrated microbiology and metabolomics analysis reveal plastic mulch film residue affects soil microorganisms and their metabolic functions. J Hazard Mater. 2022;423:127258.
80. Xie H, Wei C, Wang W, Chen R, Cui L, Wang L, Chen D, et al. Screening the phytotoxicity of micro/nanoplastics through non-targeted metallomics with synchrotron radiation X-ray fluorescence and deep learning: taking micro/nano polyethylene terephthalate as an example. J Hazard Mater. 2024;463:132886.

81. Wang QY, Liu JS, Hu B. Integration of copper subcellular distribution and chemical forms to understand copper toxicity in apple trees. Environ Exp Bot. 2016;123:125–31.
82. van de Mortel JE, Almar Villanueva L, Schat H, Kwekkeboom J, Coughlan S, Moerland PD, et al. Large expression differences in genes for iron and zinc homeostasis, stress response, and lignin biosynthesis distinguish roots of Arabidopsis thaliana and the related metal hyperaccumulator Thlaspi caerulescens. Plant Physiol. 2006;142:1127–47.

Figures

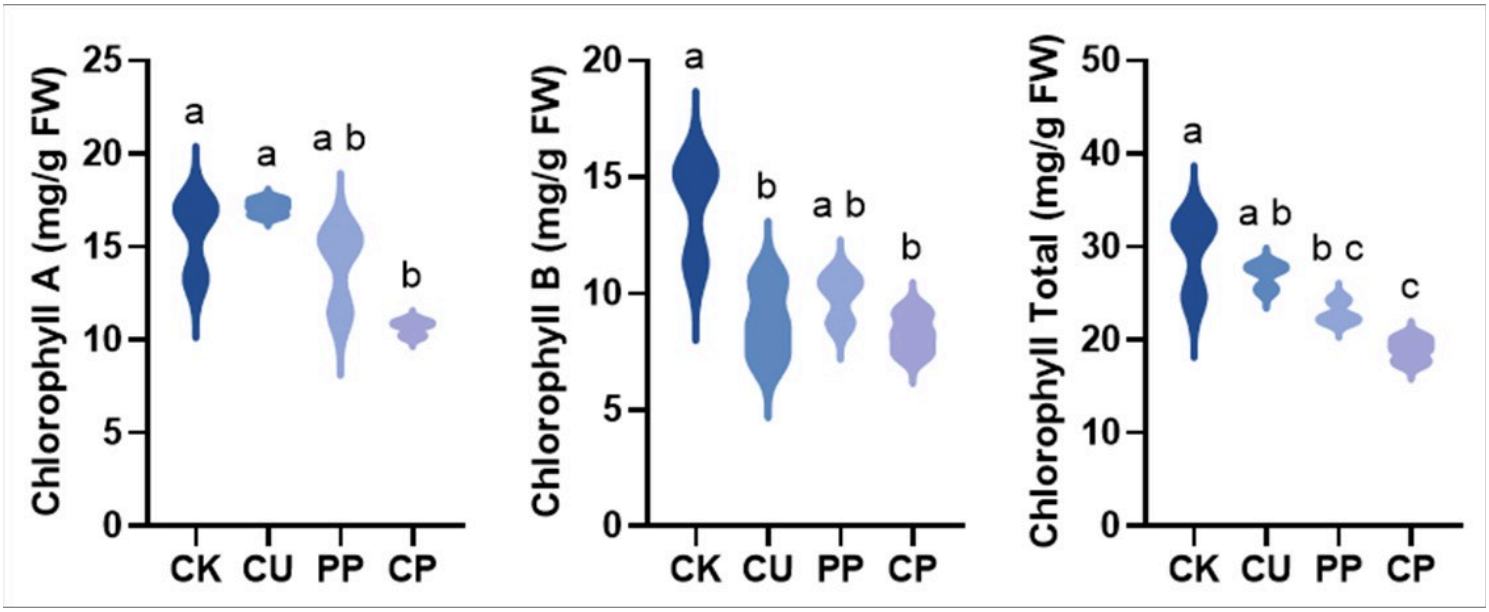


Figure 1

Changes in Chl a, Chl b, and Total Chl contents in leaves of Nymphaea ‘Black Beauty’ under CK, CU, PP, and CP treatments. Data are means ± SD, n = 3. Different lowercase letters indicate significant differences at $P < 0.05$.

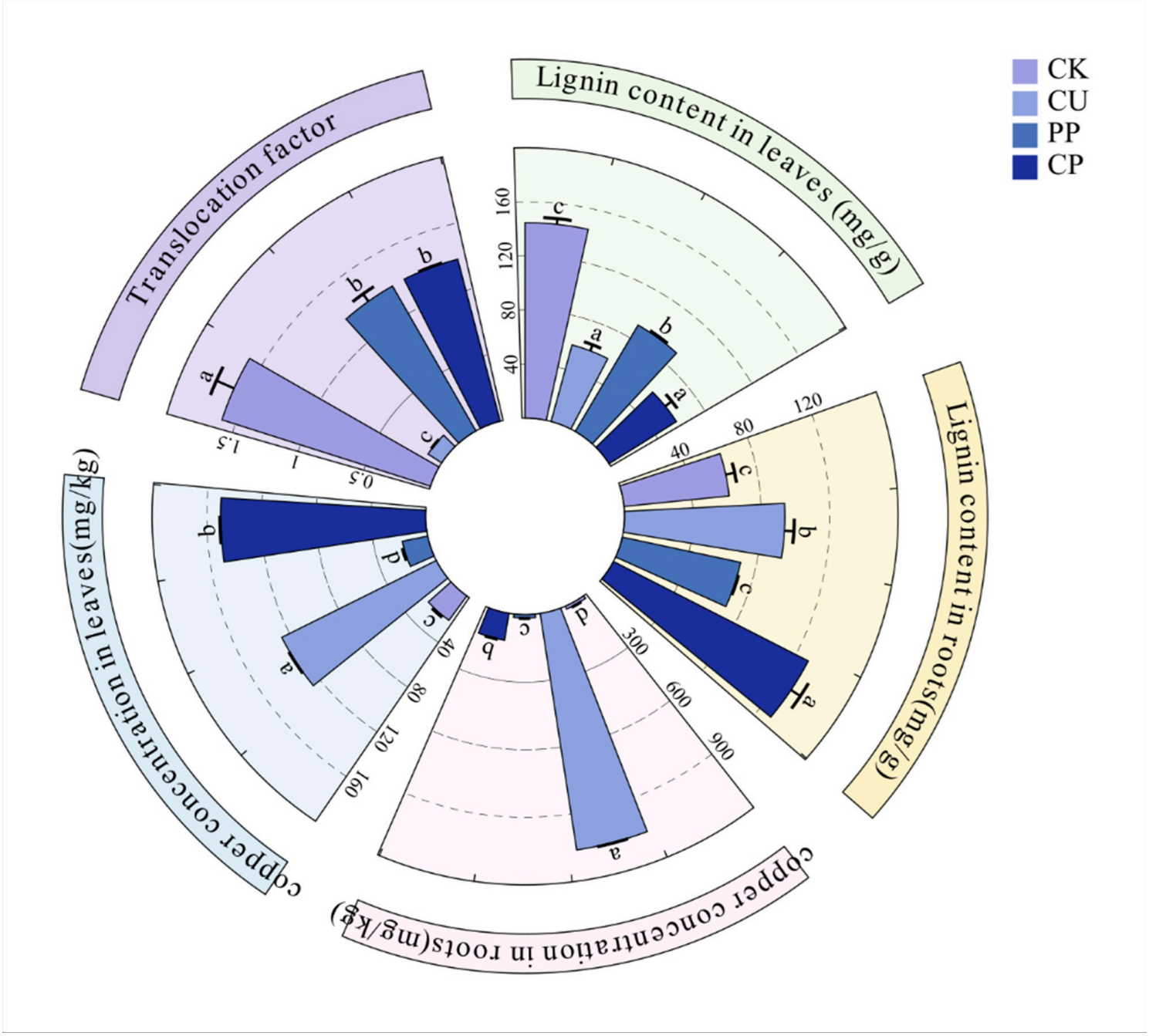


Figure 2

Changes in Cu accumulation, root-to-leaf translocation, and root/leaf lignin contents in Nymphaea ‘Black Beauty’. TF was calculated as the ratio of leaf Cu concentration to root Cu concentration. Data are means ± SD, n = 3. Different lowercase letters indicate significant differences at $P < 0.05$.

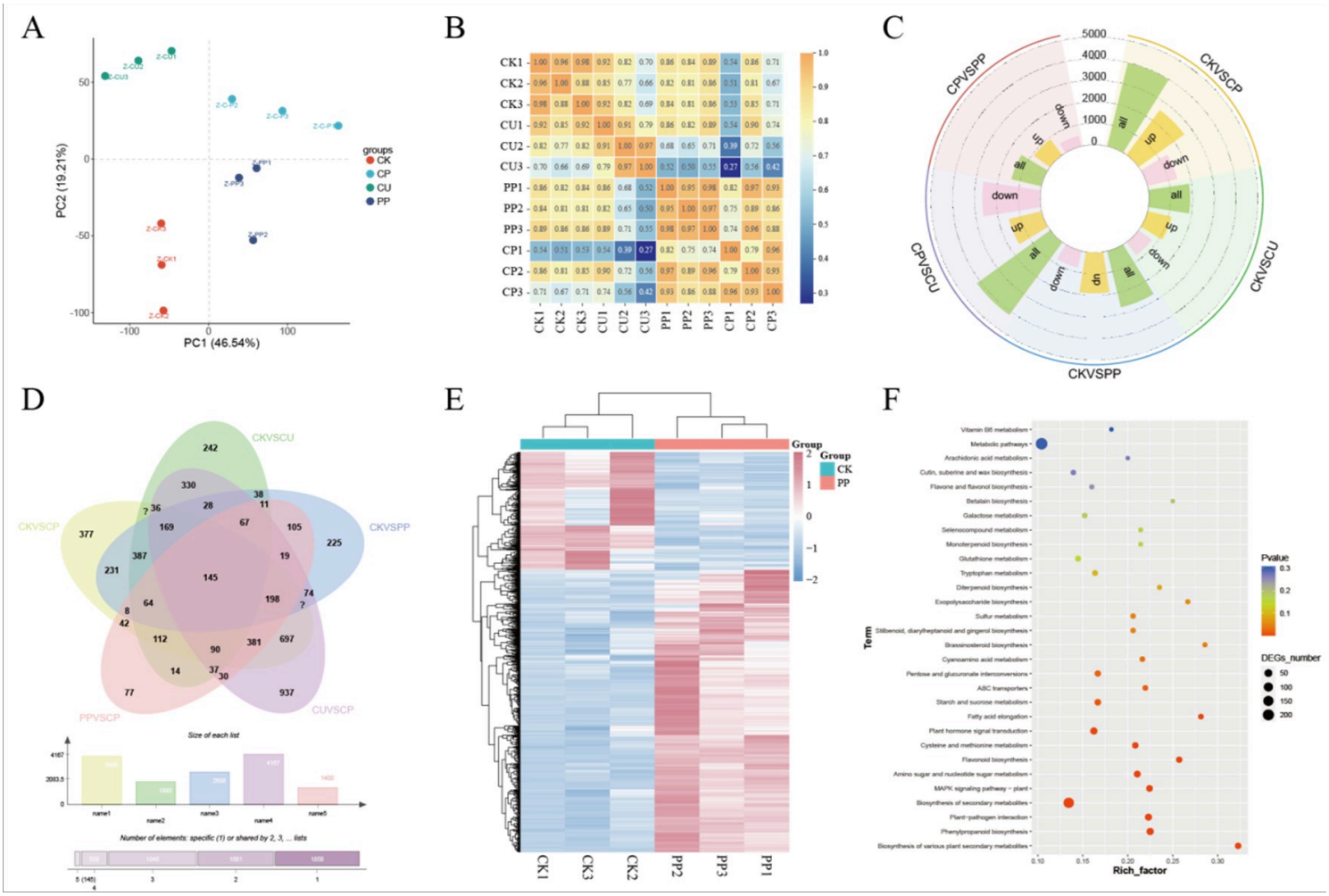


Figure 3

Transcriptome-wide separation, DEG patterns, and KEGG enrichment in leaves of Nymphaea ‘Black Beauty’. (A) PCA score plot. (B) Sample correlation heatmap. (C) Numbers of upregulated and downregulated DEGs. (D) Shared and treatment-specific DEGs. (E) Cluster heatmap of representative DEGs. (F) KEGG enrichment bubble plot.

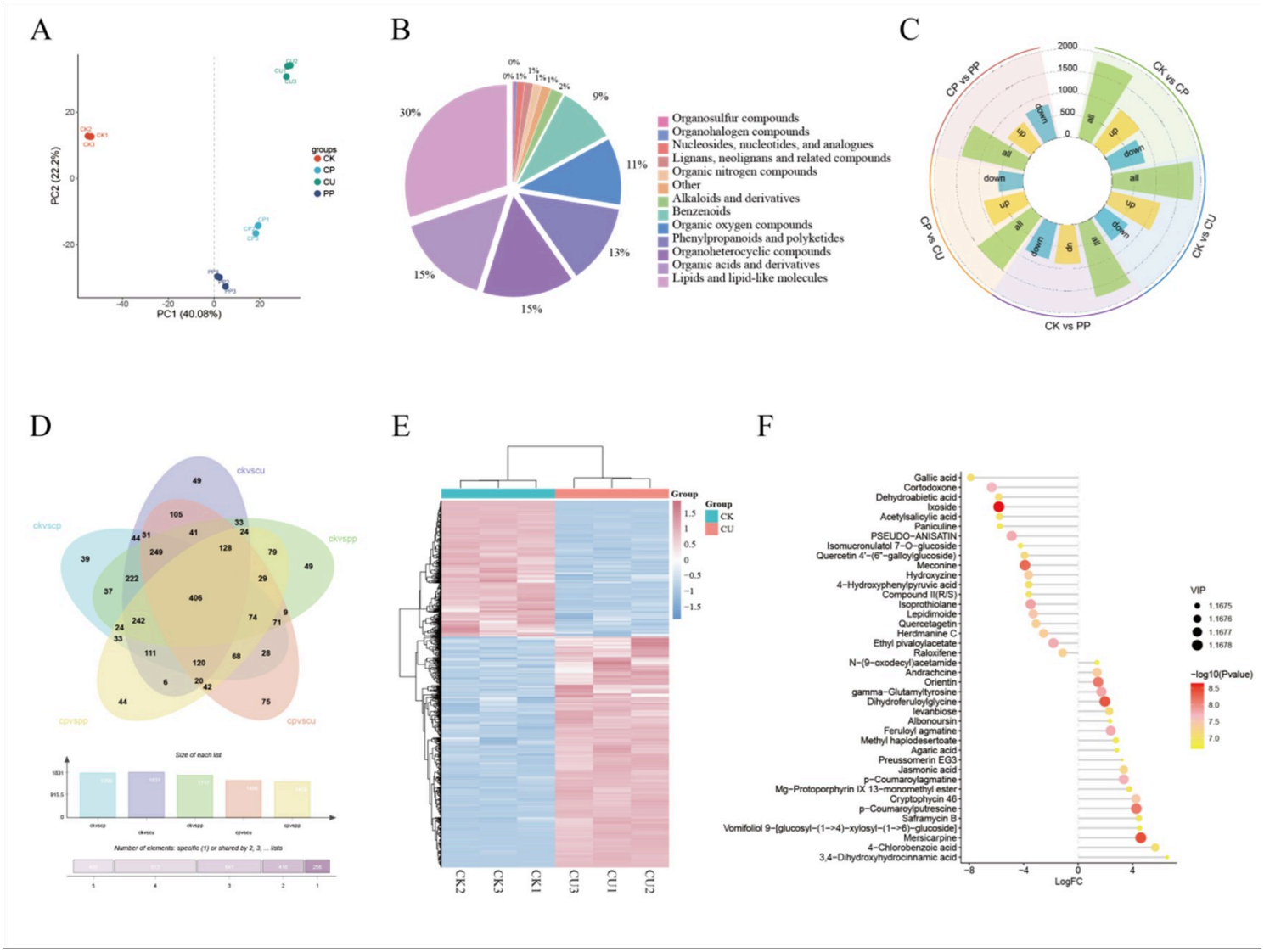


Figure 4

Untargeted metabolomic separation, DAM composition, and key metabolite screening in leaves of Nymphaea 'Black Beauty'. (A) PCA score plot. (B) Chemical classification of DAMs. (C) Major chemical classes. (D) Shared and treatment-specific DAMs. (E) DAM cluster heatmap. (F) Key DAM screening.

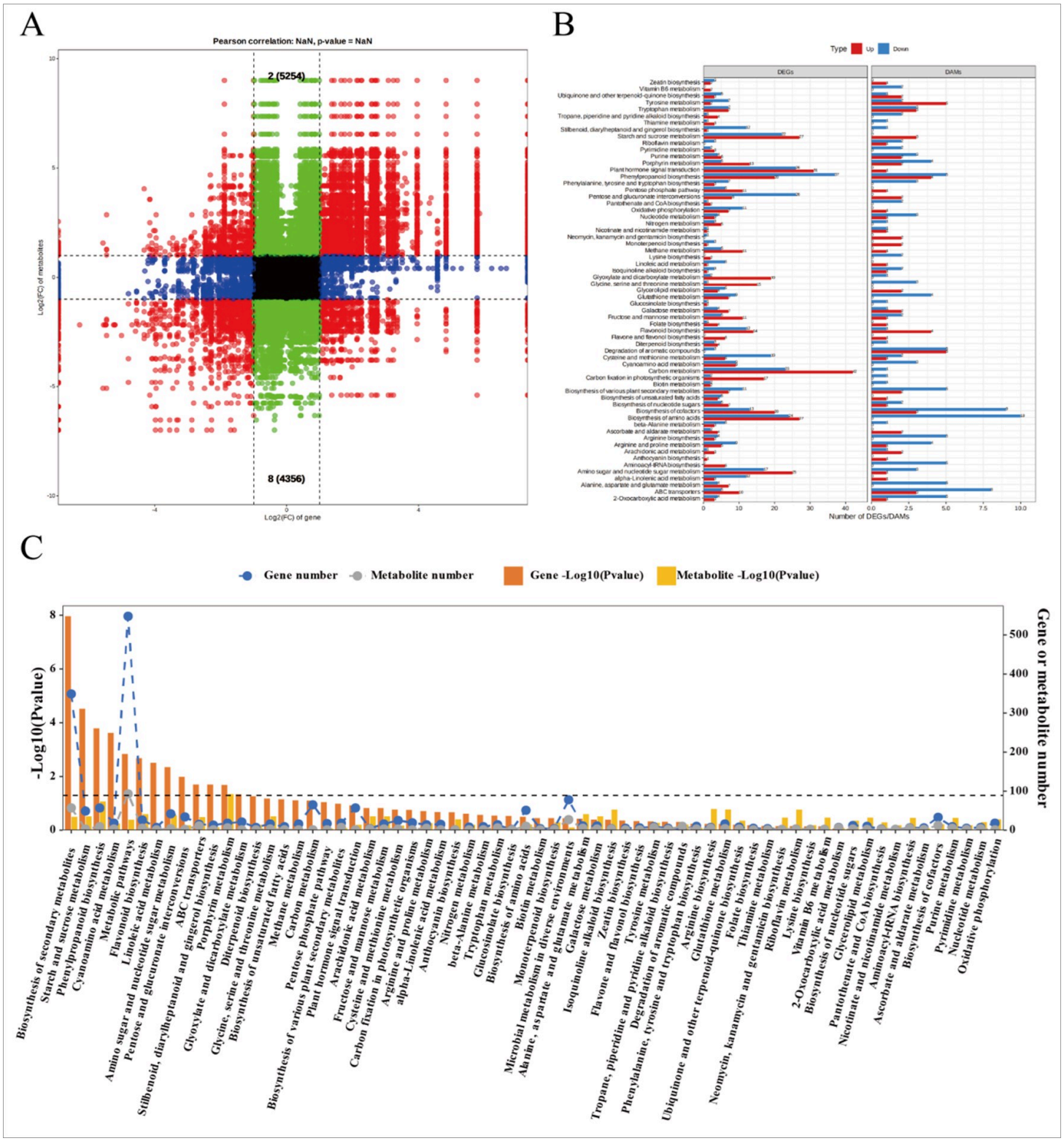


Figure 5

Integrated transcriptomic and metabolomic analysis of leaves of Nymphaea ‘Black Beauty’. (A) Nine-quadrant distribution of DEGs and DAMs. (B) Upregulated and downregulated DEGs and DAMs in KEGG pathways. (C) Joint KEGG enrichment analysis.

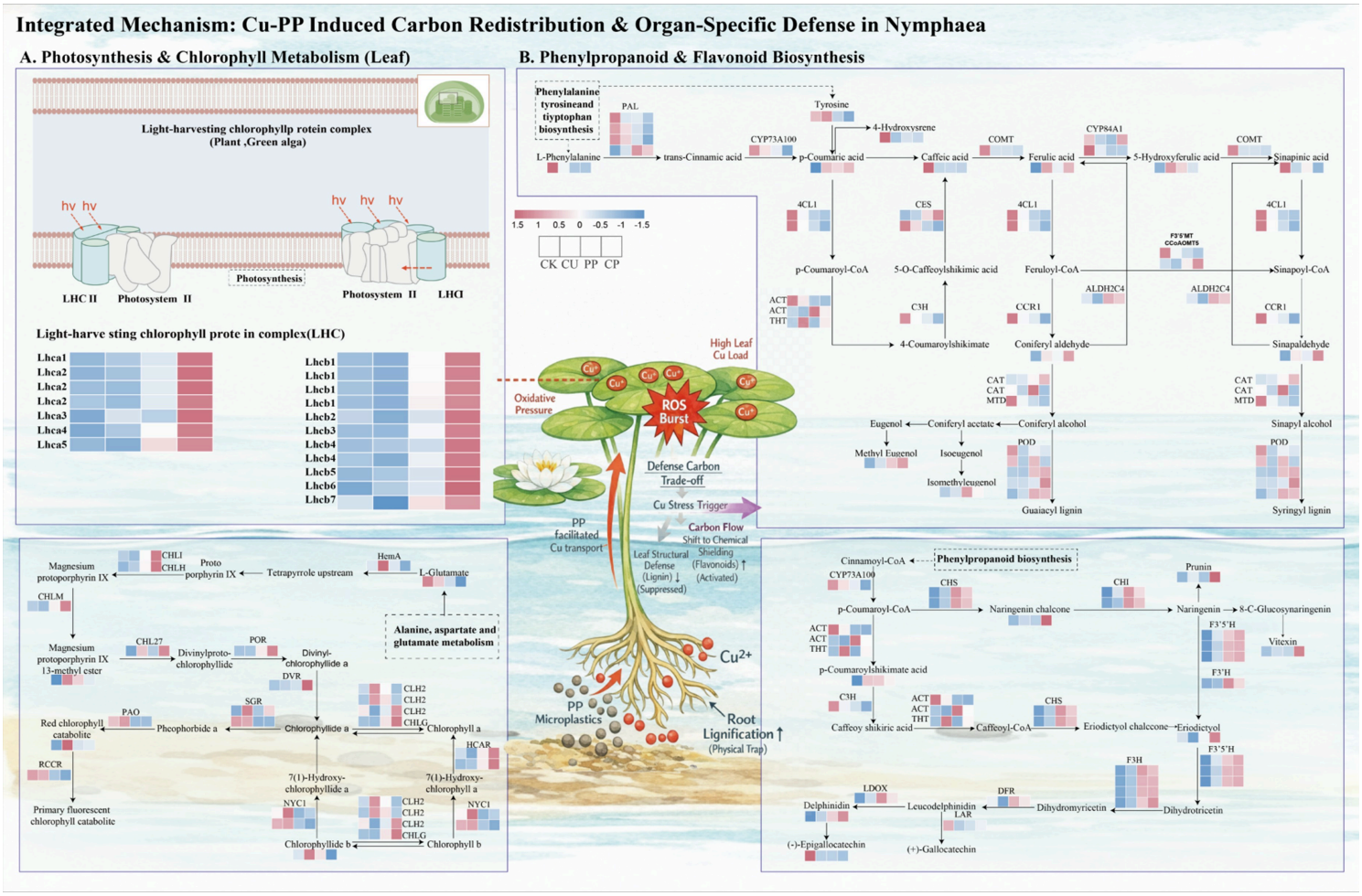


Figure 6

Integrated mechanistic model of carbon allocation remodeling and organ-specific defense in Nymphaea ‘Black Beauty’ under Cu–PP combined stress. (A) Genes and metabolites related to light-harvesting complexes, porphyrin metabolism, and chlorophyll metabolism. (B) Key genes and metabolites involved in phenylpropanoid and flavonoid biosynthesis.

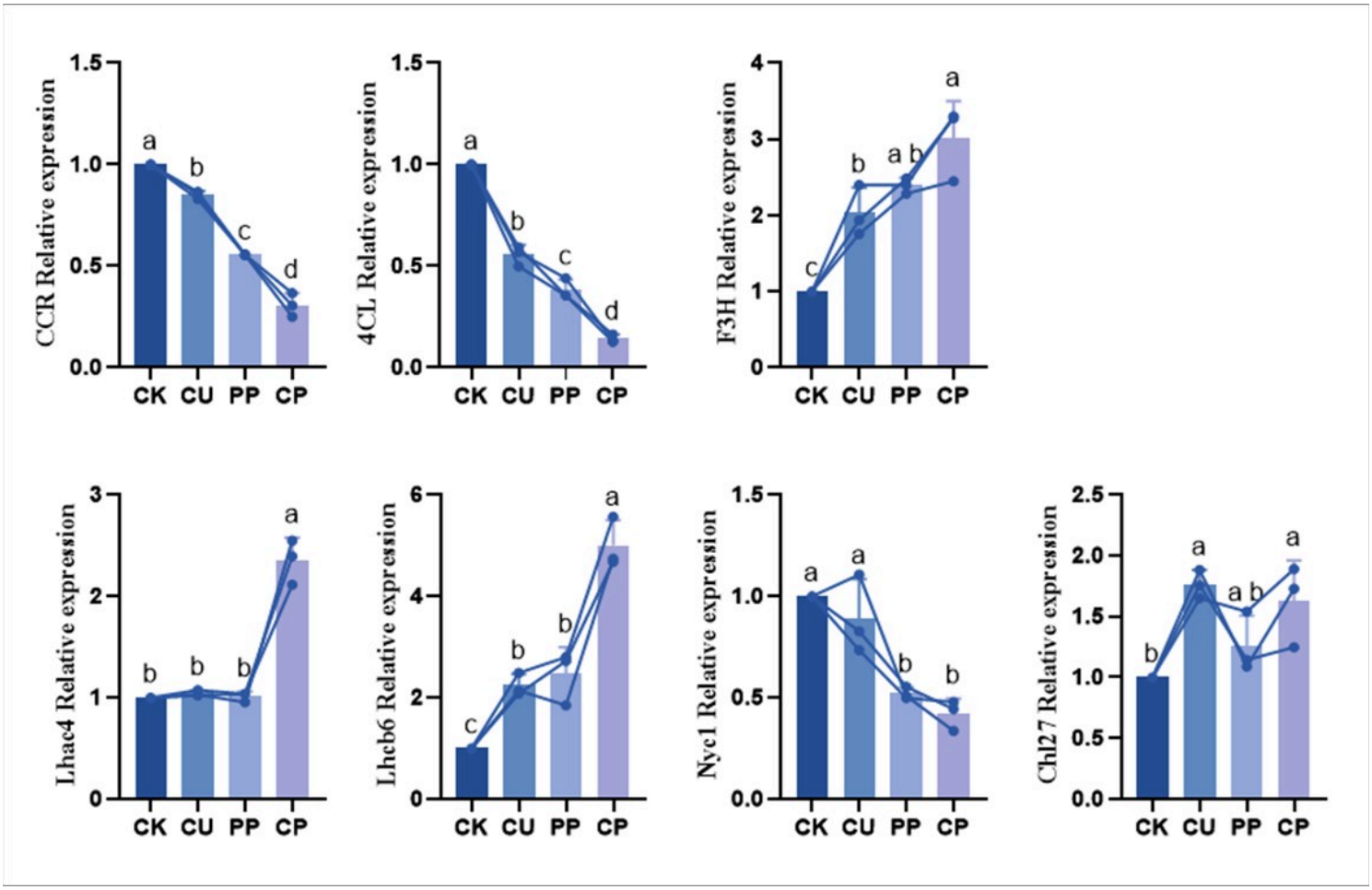


Figure 7

qRT-PCR validation of relative expression levels of key candidate genes under different treatments. Expression levels were calculated using the $2^{-\Delta\Delta Ct}$ method and normalized to CK. Data are means ± SD, n = 3. Different lowercase letters indicate significant differences at $P < 0.05$..

Supplementary Files

This is a list of supplementary files associated with this preprint. Click to download.

- SupplementaryTableS1S9.docx